Available online at www.sciencedirect.com
SCIENCE DIRECT
Polymer 46 (2005) 9533–9537
polymer
www.elsevier.com/locate/polymer

Polymer Communication

Assessing organo-clay dispersion in polymer layered silicate nanocomposites: A SAXS approach

Valerio Causin[a,*], Carla Marega[a], Antonio Marigo[a], Giuseppe Ferrara[b]

[a]*Dipartimento di Scienze Chimiche and INSTM Research Unit, Università di Padova, via Marzolo 1, 35131 Padova, Italy*
[b]*Basell Poliolefine Italia SpA—Centro Ricerche 'Giulio Natta', P.le Donegani 12, 44100 Ferrara, Italy*

Received 20 July 2005; accepted 10 August 2005

Abstract

A SAXS method for the quantitative assessment of the morphology of polymer layered silicate nanocomposites is proposed. Fitting the SAXS patterns, the number of clay layers, the periodicity of the layers in the tactoids, the thickness of the regions interposed between the clay platelets and their distributions can be measured. A good agreement with TEM data was obtained, avoiding the inconsistencies with microscopical observations often reported in the literature.

Keywords: Nanocomposites; Small-angle X-ray scattering (SAXS); Transmission electron microscopy (TEM)

1. Introduction

The dispersion of the organo-clay filler in polymer layered silicate nanocomposites (PLSN's) plays a key role in determining the property enhancement that makes these materials attractive to both industry and academia. Traditionally, the characterization of the structure and morphology of PLSN's is carried out by wide-angle X-ray diffraction (WAXD) and by transmission electron microscopy (TEM). TEM allows an evaluation by direct visualization of the morphology of PLSN's, but a great care must be exercised in the selection of representative images. WAXD is the most frequently used technique, due to its simplicity and wide availability. The shape, position and intensity of the basal peaks may yield quantitative information on intercalated clay structures. A number of experimental parameters, particle size, defect density, strain effects and mixed layering affect WAXD data, though, leading to possible inconsistencies with microscopical observations [1–5]. Moreover, the disappearance of the clay basal peaks from the WAXD pattern cannot be considered a sufficient sign that exfoliation has occurred, unless the angular range is explored beyond the low angle limit of WAXD. Small-angle X-ray scattering (SAXS) is less frequently employed as a characterization technique [6–10], often just on a qualitative basis. X-ray diffraction methods, differently from TEM, sample the whole bulk of the sample, thus potentially giving a more generalized picture of its morphology. Being able to exploit this peculiarity at its full extent would offer a valuable tool for a thorough characterization of polymer-based nanocomposite materials. The purpose of this work was that of proposing a method of analysis of the SAXS data of PLSN's that could overcome the inconsistencies with microscopy and give information on the morphology of the filler in the composite.

2. Experimental

2.1. Samples and sample characterization

Two polypropylene/cloisite 15A nanocomposites were prepared [11] by melt mixing in a single screw extruder Moplen HP500J (Basell Polyolefins) and Abriflo 65 (Abril Industrial Waxes) as a processing aid agent. The clay was added before polymer melting (sample A) in the main port of the extruder, or after polymer melting (sample B) in a second feeding port following the main one, in order to

* Corresponding author. Tel.: +39 49 8275153; fax: +39 49 8275161.
E-mail address: valerio.causin@unipd.it (V. Causin).

0032-3861/$ - see front matter © 2005 Elsevier Ltd. All rights reserved.
doi:10.1016/j.polymer.2005.08.034

obtain a different degree of intercalation between matrix and filler. TEM analyses were performed by a TECNAI 10 FEI. Samples were stained by RuO_4 and cryomicrotomed in 100 nm thick sections. Image analysis was performed with IM500 software (Leica) and approximately 200 data were collected for each sample. The results were reported in form of histograms and, by fitting with a Gaussian function, the mean and the corresponding standard deviation were calculated. SAXS spectra of both samples were acquired by a MBraun system, using Cu K_α radiation from a Philips PW 1830 X-ray generator. The data were collected by a position sensitive detector, in the scattering angular range 0.1–5.0° 2θ and they were successively corrected for blank scattering, desmeared and Lorentz-corrected. WAXD patterns were recorded by a Philips X'Pert PRO diffractometer equipped with a graphite monochromator on the diffracted beam (Cu K_α radiation) in the angular range 1.5–40° 2θ.

2.2. SAXS data treatment

A fitting method of SAXS patterns was developed on the basis of a theoretical model [12–15] in which the PLSN structure is represented by high density clay layers alternated by low density matter, either polymer or compatibilizing agent. The lateral width of the clay stacks was assumed to be much larger than its thickness [1,3,4,16], so a one-dimensional variation was considered for electron density.

The effects on the SAXS patterns of second-kind distortions was considered on the basis of the Vonk's formula [17]:

$$\gamma(x) = \gamma^0(x)\exp\left(\frac{-2x}{d}\right) \tag{1}$$

where $\gamma(x)$ and $\gamma^0(x)$ are the one-dimensional correlation functions for the distorted and ideal model, respectively, x is the distance perpendicular to the lamellar surface and d is the distortion length [17]: The value of d increases with decreasing bending of the layers. According to the Wiener–Khintchine theorem [18], the one dimensional SAXS intensity function [$I(s)$, where $s = 2\sin\theta/\lambda$, 2θ is the diffraction angle and λ is the radiation wavelength, i.e. in this work Cu K_α] is given as the Fourier cosine transform of the $\gamma(x)$ function:

$$I(s) = F_c\left[\gamma^0(x)\exp\left(\frac{-2x}{d}\right)\right] = F_c[\gamma^0(x)] * F_c\left[\exp\left(\frac{-2x}{d}\right)\right] \tag{2}$$

where $F_c[\ ]$ and the asterisk denote the Fourier cosine and the convolution, respectively, so

$$I(s) = I^0(s) * \left[\frac{2/d}{s^2 + (2/d)^2}\right] \tag{3}$$

where $I^0(s)$ is the one dimensional SAXS intensity for the ideal lamellar structure [13]:

$$I^0(s) = I^{\mathrm{I}}(s) + I^{\mathrm{II}}(s) \tag{4}$$

where:

$$I^{\mathrm{I}}(s) = \frac{(\rho_Y - \rho_Z)^2}{4\pi^2 s^2 X} \times \frac{|1-F_Y|^2(1-|F_Z|^2) + |1-F_Z|^2(1-|F_Y|^2)}{(1-F_Y F_Z)^2} \tag{5}$$

$$I^{\mathrm{II}}(s) = \frac{(\rho_Y - \rho_Z)^2}{2\pi^2 s^2 X N} \times \mathrm{Re}\left\{\frac{F_Z(1-F_Y)^2(1-(F_Y F_Z)^N)}{(1-F_Y F_Z)^2}\right\} \tag{6}$$

In these equations, F_Y and F_Z represent the Fourier transforms of the distribution functions of the clay layers (Y) and of the low-density regions interposed between the clay platelets (Z), ρ_Y and ρ_Z are the electron densities of the clay and low-density regions, respectively, N is the number of layers and X the average long period. The thickness Y of the alumino–silicatic layers was fixed in 1.0 nm [19].

3. Results and discussion

Fig. 1 shows the TEM general view of the samples considered in this paper to validate the method of SAXS data analysis. As may be seen, sample B displays larger tactoids, due to the shorter residence time of the clay in the extruder, which was not long enough to allow for a sufficient homogenization of the filler.

Clay sheets, and consequently tactoids, are three dimensional and usually randomly oriented in the bulk of the material. The samples taken to be analyzed by TEM came from random locations inside the specimens, thus giving a general picture of its morphology.

A problem that may arise with TEM micrographs is that when the layers in the tactoids are not in the edge-on position, the contrast between adjacent layers is altered and thus they cannot be properly distinguished [9].

In Fig. 1, the coexistence of well defined layered stacks and dark regions can be seen, confirming that the tactoids are indeed randomly oriented in the space. This is a quite important observation, because the isotropicity of the spatial distribution of the scattering elements is required for a meaningful SAXS analysis. Fig. 2 shows some examples of the high magnification TEM micrographs used for the quantification of the samples' morphology. The single layers composing the tactoids can be clearly distinguished and so it was possible to evaluate the mean number (N_{TEM}) and periodicity (X_{TEM}) of the individual clay platelets in the tactoids. Only tactoids with layers in the edge-on position were considered for quantification. The periodicity was

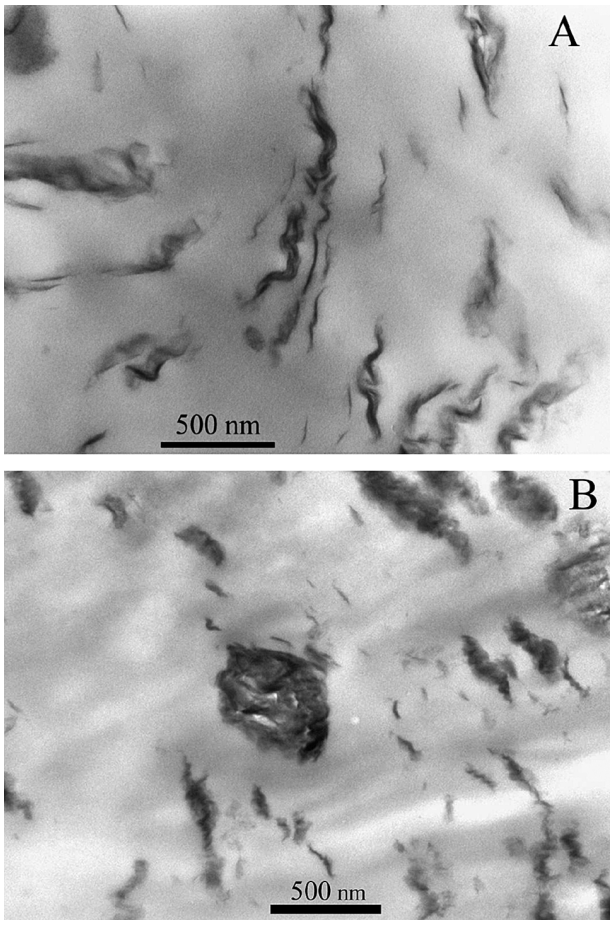

Fig. 1. TEM micrographs of sample A (top) and B (bottom).

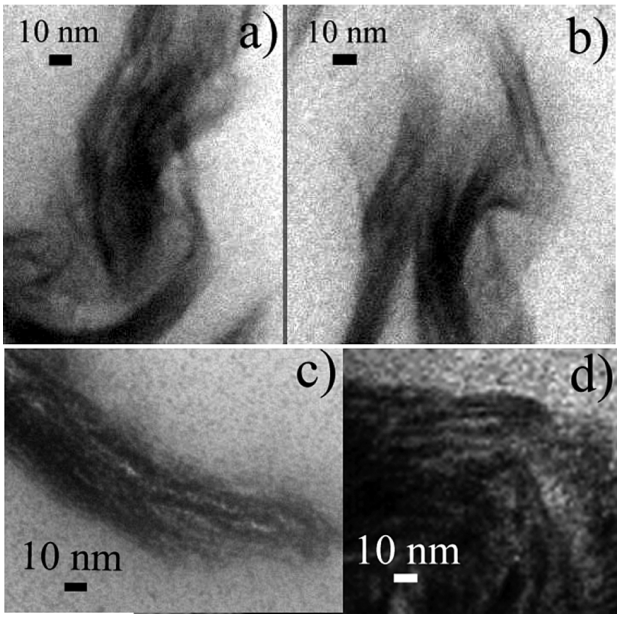

Fig. 2. High magnification TEM micrographs of samples A (a) and (b) and B (c) and (d).

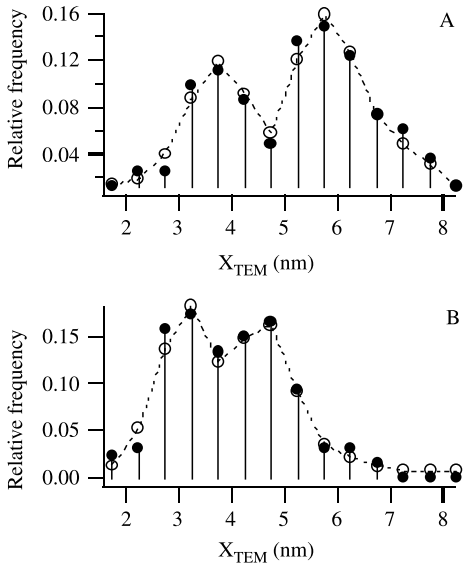

Fig. 3. Experimental histograms (●) and Gaussian fitting (○) of the periodicity of clay layers distributions determined by TEM for samples A (top) and B (bottom).

intended as the distance between the centers of two adjacent clay layers and was measured by image analysis software previously calibrated on the internal scale of the TEM micrograph. The whole range of data acquired, from 1.5 to 8.5 nm was divided into 14 intervals 0.5 nm wide and a histogram of the relative frequency of the measurements falling into each class was plotted (Fig. 3). The diagrams of Fig. 3 were fit with two Gaussian functions, in order to obtain the mean and standard deviation of each of the populations of clay layers (Table 1). A bimodal distribution was in fact observed in both samples. The first population was that of tactoids that proved immiscible with the polymer and retained the spacing of clay layers typical of pristine Cloisite 15A (3.2 nm). The second population was formed by intercalated stacks of clay layers. The intercalated clay layers appear to be more numerous and more separated in sample A (Figs. 2 and 3), suggesting that a more significant interaction of the polymer with the clay occurred as a consequence of the increased homogenization time. Samples A and B produced very similar SAXS patterns

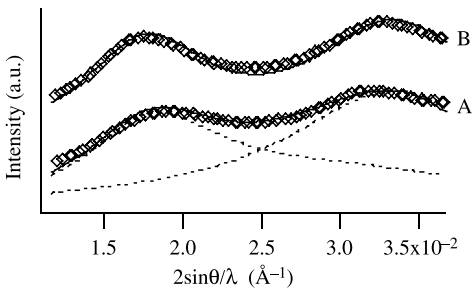

Fig. 4. Best fits between experimental and calculated SAXS patterns (◇: Experimental, solid line: Calculated). For sample A the calculated signals relative to the immiscible and intercalated populations of clay layers are also shown by dotted lines.

Table 1
Average number of clay layers (N), periodicity of the layers (X) and thickness of low density region (Z), and relative standard deviations of X (σ_X/X) and of Z (σ_Z/Z) for the two populations of tactoids in samples A and B

Sample	Tactoid population	N_{TEM}	X_{TEM} (nm)	$(\sigma_X/X)_{TEM}$	N_{SAXS}	Z_{SAXS} (nm)	X_{SAXS} (nm)	$(\sigma_Z/Z)_{SAXS}$	$(\sigma_X/X)_{SAXS}$
A	Immiscible	11	4	0.23	11	2	3	0.38	0.28
A	Intercalated	11	6	0.15	10	4	5	0.40	0.33
B	Immiscible	10	3	0.26	10	2	3	0.39	0.34
B	Intercalated	10	5	0.20	13	4	5	0.25	0.20

Subscript TEM denotes data evaluated by the analysis of TEM micrographs, subscript SAXS indicates those assessed by fitting of the SAXS patterns.

with two maxima, approximately at 0.018 and 0.032 $Å^{-1}$ (Fig. 4). Coexistence of different dispersion morphologies has been reported in the literature [8]. The SAXS patterns were fitted by the method proposed and the morphological data obtained are shown in Table 1. As can be seen, a good agreement with TEM was observed. It is especially interesting to note that usually inconsistencies are found between TEM and X-ray diffraction concerning the number of platelets in the stacks. This is due to the fact that the particles seen in micrographs can consist of face–face aggregation of crystallites, as reported by Vaia [7] and by other authors as well [1,3,20]. Our model could reproduce the real number of clay layers in tactoids because it considered possible second-kind distortions [15,17]. As may be seen in Fig. 5, in fact, when face-to-face aggregation occurs, slight differences in the stacking directions may appear. In this case, WAXD detects each tactoid as a separate crystallite, while if a distortion parameter were introduced in the SAXS analysis, aggregated tactoids are considered as a single stack.

If ideal and undistorted lamellar structures were postulated [11,13], the fitting of SAXS patterns yielded 5 platelets for each tactoid of sample B and 4 and 5 layers, respectively, for the immiscible and intercalated tactoids of sample A. This result was also confirmed by WAXD. The crystallite size (L_{001}) of unintercalated tactoids was estimated by the Scherrer equation [16]: Dividing L_{001} by the periodicity d_{001} of the clay basal peak, the number of layers (N_{WAXD}) constituting the unintercalated stacks could be assessed. The N_{WAXD} obtained with this method were four for sample A and five for sample B, in good accord with those calculated by the SAXS analysis with undistorted layers, but in disagreement with TEM and SAXS data yielded by fitting on the basis of the distorted layer model. These results supported the hypothesis that clay stacks, either intercalated or not, that were observed by TEM in our PP/montmorillonite composites, were composed of crystallites aggregated face-to-face.

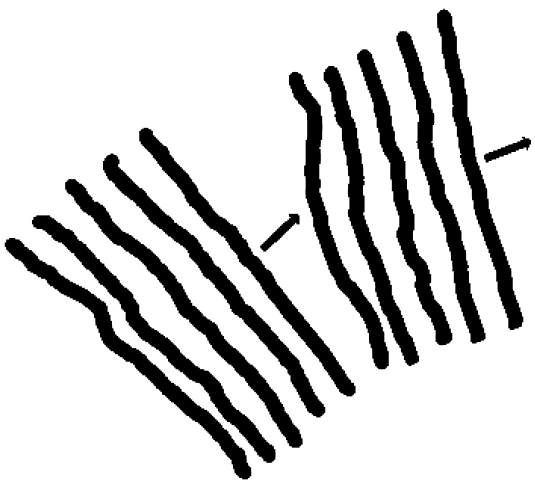

Fig. 5. Scheme of two clay tactoids aggregated face-to-face. Arrows indicate the stacking direction.

4. Conclusion

A SAXS fitting method for the quantitative assessment of the morphology of clay in polymer layered silicate nanocomposites was proposed. Data were in good agreement with TEM, thus the inconsistencies with microscopical observations often reported in the literature, due to flocculation or face-to-face aggregation of the clay layers, were avoided. This calls for consideration of an accurate and quantitative SAXS analysis to complement and enrich the traditional morphological investigation of nanocomposites made by TEM and WAXD.

Acknowledgements

This work was carried out in the context of the European Network of Excellence Nanofun-Poly. V.C. gratefully acknowledges financial support by Basell Italia S.p.A., through a Federchimica grant.

References

[1] Ranade A, D'Souza NA, Gnade B. Polymer 2002;43:3759–66.
[2] Vaia RA, Liu W. J Polym Sci, Polym Phys Ed 2002;40:1590–600.
[3] Ray SS, Okamoto M. Macromol Rapid Commun 2003;24:815–40.
[4] Eckel DF, Balogh MP, Fasulo PD, Rodgers WR. J Appl Polym Sci 2004;93:1110–7.
[5] Morgan AB, Gilman JW. J Appl Polym Sci 2003;87:1329–38.
[6] Gelfer MY, Song HH, Liu L, Hsiao BS, Chu B, Rafailovich M, Si M, Zaitsev V. J Polym Sci, Polym Phys Ed 2003;41:44–54.

[7] Vaia RA, Liu W, Koerner H. J Polym Sci, Polym Phys Ed 2003;41: 3214–36.
[8] Koo CM, Kim SO, Chung IJ. Macromolecules 2003;36:2748–57.
[9] Yoonessi M, Toghiani H, Daulton TL, Lin J-S, Pittman CU Jr. Macromolecules 2005;38:818–31.
[10] Ristolainen N, Vainio U, Paavola S, Torkkeli M, Serimaa R, Seppälä J. J Polym Sci, Polym Phys Ed 2005;43:1892–903.
[11] Benetti EM, Causin V, Marega C, Marigo A, Ferrara G, Ferraro A, Consalvi M, Fantinel F. Polymer 2005;46:8275–85.
[12] Blundell DJ. Polymer 1978;19:1258–66.
[13] Marega C, Marigo A, Cingano G, Zannetti R, Paganetto G. Polymer 1996;37:5549–57.
[14] Marigo A, Marega C, Zannetti R, Sgarzi P. Eur Polym J 1998;34: 597–603.
[15] Marega C, Marigo A, Causin V. J Appl Polym Sci 2003;90:2400–7.
[16] Ray SS, Okamoto M, Okamoto M. Macromolecules 2003;36: 2355–67.
[17] Vonk CG. J Appl Cryst 1978;11:541–6.
[18] Sasanuma Y, Abe A, Sasanuma T, Kitano Y, Ishitani A. J Polym Sci, Polym Phys Ed 1993;31:1179–86.
[19] Shao W, Wang Q, Ma H. Polym Int 2005;54:336–41.
[20] Nam PH, Fujimori A, Masuko T. J Appl Polym Sci 2004;93:2711–20.